AJNR

Contrast-Enhanced MR Angiography at 3T in the Evaluation of Intracranial Aneurysms: A Comparison with Time-of-Flight MR Angiography

K. Nael, J.P. Villablanca, R. Saleh, W. Pope, A. Nael, G. Laub and J.P. Finn

AJNR Am J Neuroradiol 2006, 27 (10) 2118-2121
http://www.ajnr.org/content/27/10/2118

TECHNICAL NOTE

Contrast-Enhanced MR Angiography at 3T in the Evaluation of Intracranial Aneurysms: A Comparison with Time-of-Flight MR Angiography

K. Nael
J.P. Villablanca
R. Saleh
W. Pope
A. Nael
G. Laub
J.P. Finn

SUMMARY: The combination of 3T and parallel-acquisition techniques holds promise for improved performance of contrast-enhanced MR angiography (MRA), in terms of speed, spatial resolution, and coverage. We present a comparison of 2 MRA techniques, including time-of-flight (TOF) and contrast-enhanced MRA, for detection and evaluation of intracranial aneurysms. Our results show that contrast-enhanced MRA with highly accelerated parallel acquisition at 3T does not have the known drawbacks of TOF-MRA techniques, including prolonged acquisition time, spin saturation, and flow-related artifacts, with comparable aneurysm characterization.

Despite the promising results of time-of-flight MR angiography (TOF-MRA) for evaluation of intracranial aneurysms,[1,2] disadvantages include spin saturation and phase dispersion due to slow or turbulent flow[3,4] and long acquisition times, typically lasting several minutes.

Contrast-enhanced MRA can address these limitations and has already shown promise for evaluation of intracranial aneurysms.[5,6] However, the competing requirements for coverage and acquisition speed generally force a compromise in spatial resolution relative to TOF-MRA.

The broad availability of 3T MR imaging systems with higher available signal-to-noise ratios (SNRs) and the introduction of parallel imaging [7-9] have significantly enhanced the performance of MRA techniques in evaluation of cerebrovascular disease.[10,11]

If its potential is realized, contrast-enhanced MRA at 3T might achieve a spatial resolution and image quality that rivals TOF-MRA, without the known drawbacks. The purpose of this study was to evaluate a high-spatial-resolution contrast-enhanced MRA protocol, integrated with highly accelerated parallel acquisition for visualization and characterization of intracranial aneurysms, and to compare the results with a more standard clinical routine (TOF-MRA) at 3T, in a population of patients with known intracranial aneurysms.

Methods

Fifteen patients (2 men, 13 women; age range, 46–83 years) with known intracranial aneurysms were prospectively scanned by using high-spatial-resolution 3D MRA at 3T, including both TOF and contrast-enhanced MR imaging techniques. All MRA studies were performed on a 3T whole-body MR imaging system (Magnetom Trio, Siemens Medical Solutions, Erlangen, Germany) by using an 8-channel Neurovascular Array Coil (Inviro, Orlando, Fla) for signal cross intensity reception.

Multislab TOF-MRA was performed with 4 axial slabs of 40 sections per slab, with 0.9-mm-thick spanning from the skull base to the midsylvian region. The sequence parameters were the following: TR/TE, 20/3.2 ms; flip angle (FA), 20°; sampling bandwidth (BW), 200 Hz/pixel; field of view, 210 × 180 mm; and image matrix, 448 × 307. Parallel imaging was performed with a generalized autocalibrating partially parallel acquisition with an acceleration factor of 2 (GRAPPA ×2). These settings resulted in acquisition of 3D data with $0.6 \times 0.5 \times 0.9$ mm^3 voxels in 5 minutes 40 seconds.

Subsequently, high-spatial-resolution contrast-enhanced MRA was performed in the coronal plane following injection of 0.15 mmol/kg of gadodiamide. A fast-spoiled gradient-refocused echo sequence (TR/TE, 3/1.2 ms; FA, 20°; BW, 720 Hz/pixel; field of view, 360 × 240 mm; and image matrix, 576 × 334) was used for image acquisition. An asymmetric *k*-space sampling scheme (partial Fourier, 80%) in all 3 planes and parallel acquisition with an acceleration factor of 4 (GRAPPA ×4) were used. By selecting 100 partitions with a thickness of 0.8 mm, contrast-enhanced MRA of the entire carotid and vertebrobasilar circulation was performed during a 20-second acquisition, with acquired voxel dimensions of $0.7 \times 0.6 \times 0.8$ mm^3.

Image analysis was performed independently and in random order by 2 experienced neuroradiologists on a commercially available 3D workstation. The overall image quality was analyzed with regard to arterial enhancement, presence of artifacts (including parallel acquisition reconstruction artifact and motion artifact) or saturation artifact, and/or noise, by using a 1–3 scoring scale (1, poor image quality and arterial enhancement and/or presence of significant amount of artifacts/noise impairing the diagnosis; 2, good image quality and arterial enhancement and/or mild-to-moderate amount of artifacts/noise not interfering with diagnosis; and 3, excellent image quality for highly confident diagnosis with none-to-minimal amount of artifacts/noise).

For evaluation of aneurysms, the observers were asked to grade the quality of aneurysm depiction and their diagnostic confidence for perception of aneurysm and its relation to parent vessels, by using a 3-point scale: grade 3, excellent depiction of an aneurysm, full confidence for perception of aneurysm border, and clear relationship between the aneurysm and the parent vessel; grade 2, good depiction of an aneurysm, not completely confident for the perception of aneurysm border, and/or no clear relationship with parent vessel; and grade 1, lesion scarcely visible. Maximal spheric diameters of the aneurysm sac were measured on both TOF-MRA and contrast-enhanced MRA, separately.

Received March 6, 2006; accepted after revision May 5.

From the Department of Radiological Sciences (K.N., J.P.V., R.S., W.P., A.N., J.P.F.), David Geffen School of Medicine at University of California Los Angeles, Los Angeles, Calif; and Siemens Medical Solutions (G.L.), Erlangen, Germany.

Please address correspondence to: Kambiz Nael, MD, Department of Radiological Sciences, University of California Los Angeles, 10945 Le Conte Ave, Ste 3371, Los Angeles, CA 90095-7206; e-mail: nkambiz@mednet.ucla.edu

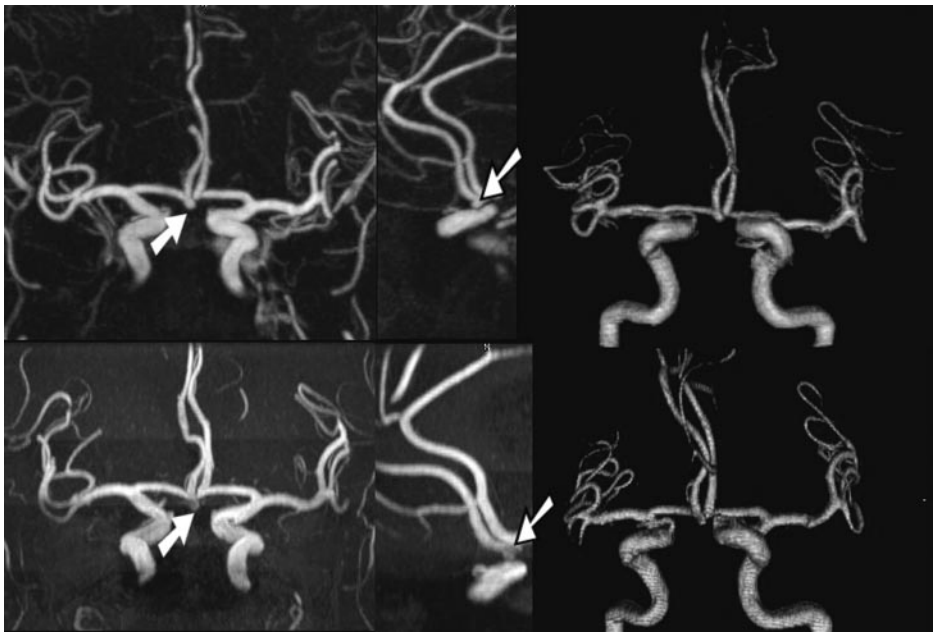

Fig 1. Coronal and sagittal oblique maximum intensity projection (MIP) and 3D volume-rendered projections from contrast-enhanced MRA (upper row) and TOF-MRA (lower row) show a small inferiorly projecting saccular aneurysm (*arrows*) in the AcomA with maximal diameter measurement of 2.6 × 3.1 mm.

Results

All studies were determined to be of diagnostic image quality by both observers. The overall image quality scores for contrast-enhanced MRA and TOF-MRA were in the diagnostic range (median, 3; range, 2–3) for both observers. There was no significant difference for image quality scores between the 2 readers or between the 2 techniques. No parallel acquisition reconstruction artifact was noted, and image noise was not found to interfere with diagnostic image quality.

Sixteen aneurysms were detected. Aneurysm locations included the supraclinoid internal carotid artery ($n = 5$), infraclinoid internal carotid artery ($n = 8$), anterior communicating (AcomA) ($n = 2$) (Fig 1), and the basilar artery ($n = 1$).

In qualitative analysis for aneurysm visualization by using contrast-enhanced MRA, both observers identified 14 aneurysms (87%) with excellent confidence (score 3) and 2 (13%) with good confidence (score 2). In a qualitative analysis for the aneurysm visualization by using TOF-MRA, both observers identified 10 aneurysms (63%) with excellent confidence (score 3) and 5 aneurysms (31%) with good confidence (score 2), whereas 1 aneurysm (6%) was scarcely visible (score 1). This was a 21-mm basilar tip aneurysm (Fig 2).

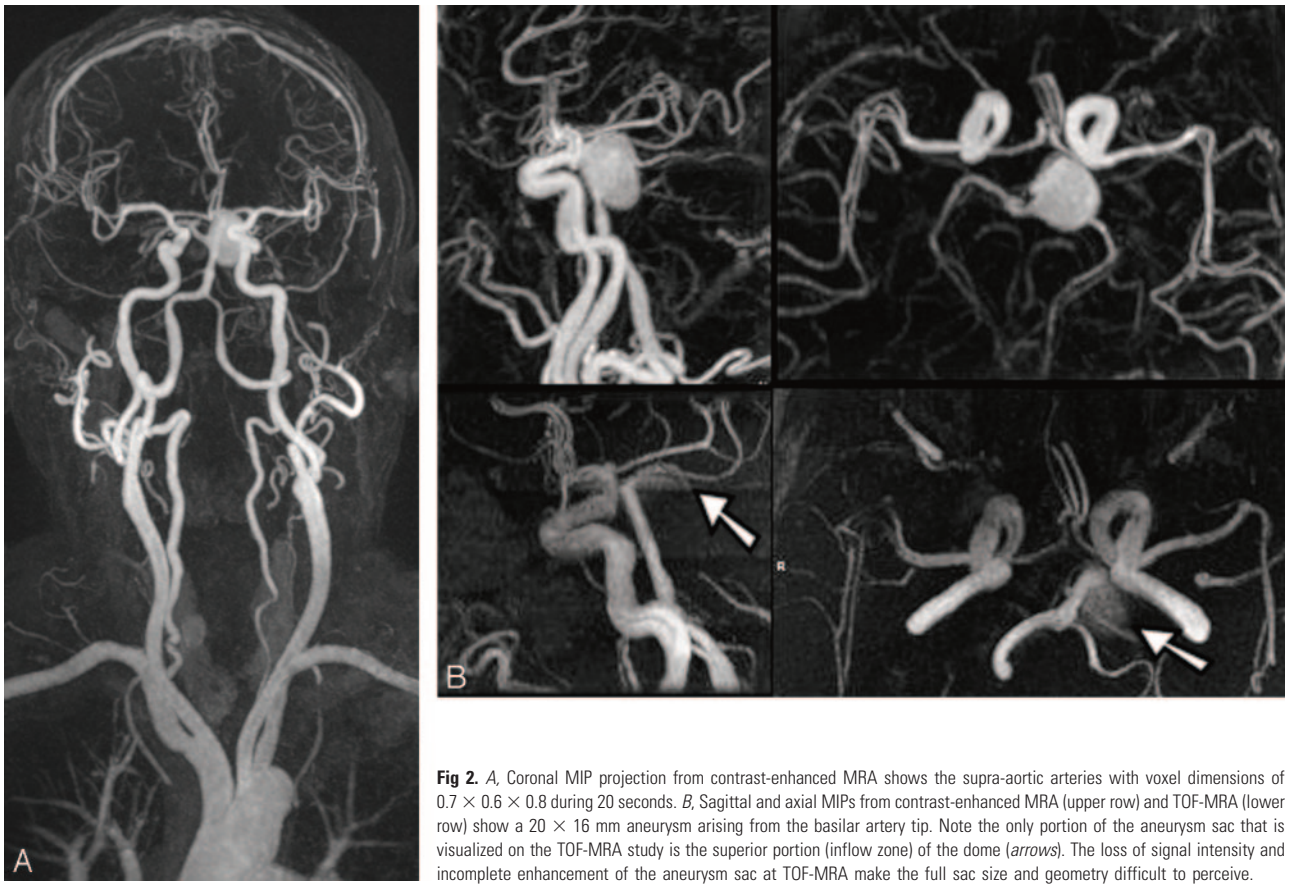

Fig 2. *A,* Coronal MIP projection from contrast-enhanced MRA shows the supra-aortic arteries with voxel dimensions of 0.7 × 0.6 × 0.8 during 20 seconds. *B,* Sagittal and axial MIPs from contrast-enhanced MRA (upper row) and TOF-MRA (lower row) show a 20 × 16 mm aneurysm arising from the basilar artery tip. Note the only portion of the aneurysm sac that is visualized on the TOF-MRA study is the superior portion (inflow zone) of the dome (*arrows*). The loss of signal intensity and incomplete enhancement of the aneurysm sac at TOF-MRA make the full sac size and geometry difficult to perceive.

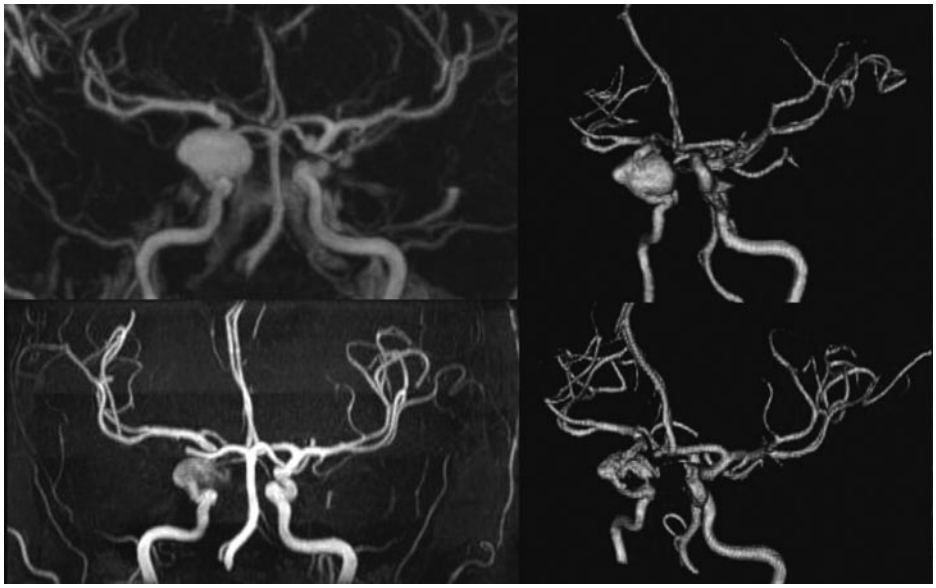

Fig 3. Coronal oblique MIP and volume-rendered projections from contrast-enhanced MRA (upper row) and TOF-MRA (lower row) show a large (16 × 12 mm) aneurysm arising from the cavernous portion of the right internal carotid artery. Note loss of signal intensity and incomplete flow-related enhancement of the aneurysm sac at TOF-MRA, which limits definition of the border of the aneurysm.

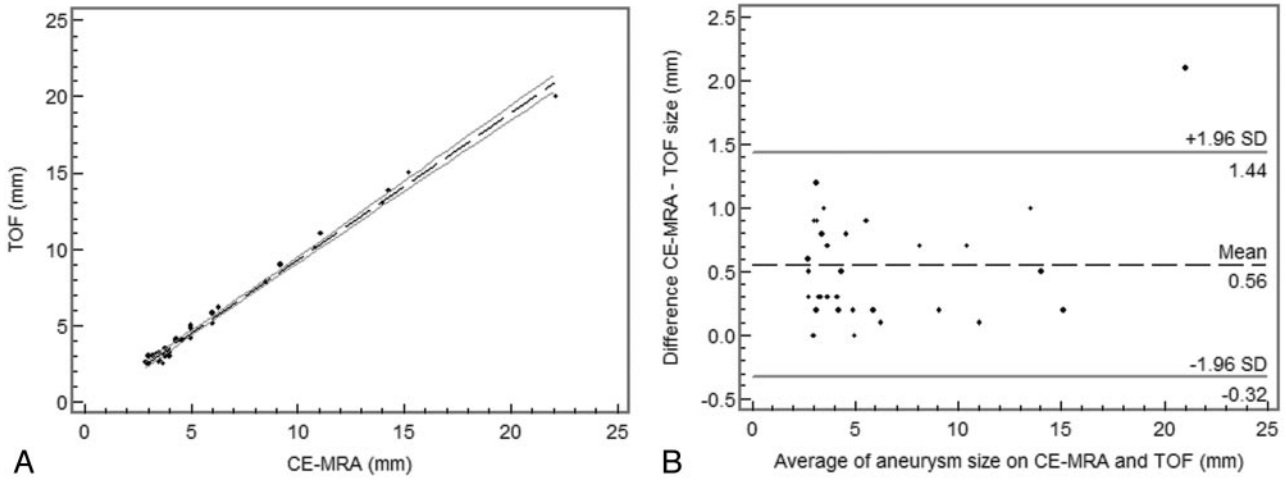

Fig 4. *A,* Scatterplot shows significant correlation (r = 0.91, 95% CI = 0.87 to 0.96) for aneurysmal dimension measurements between TOF and contrast-enhanced MRA. *B,* Bland-Altman plot shows differences of no more than 2 mm between aneurysmal dimension measurements on contrast-enhanced MRA and those on TOF-MRA.

There was excellent interobserver agreement for qualitative analysis of the aneurysm depiction and perception for both contrast-enhanced MRA ($\kappa = 1$) and TOF-MRA ($\kappa = 0.9$). However, there was a relatively high intertechnique variability ($\kappa = 0.43$) for qualitative evaluation of aneurysms. This was due to lower scores in 6/16 (37%) aneurysms on TOF-MRA, which was thought be due to the presence of intra-aneurysmal signal intensity loss (Figs 2 and 3).

For dimensional measurements, the average maximal spheric aneurysm sac diameter was 6.26 mm (range, 2.6–22.1 mm) on contrast-enhanced MRA and 5.91 mm (range, 2.4–20 mm) on TOF-MRA, with no statistically significant difference ($P = .3$). There was significant correlation for the dimensional measurements of the sac between TOF and contrast-enhanced MRA ($r = 0.91$, 95% confidence interval [CI] = 0.87 to 0.96) (Fig 4). Six aneurysms (38%) were <4 mm in maximal diameter, 6 (38%) aneurysms were between 4–10 mm in maximal diameter, and 4 (24%) were larger than 10 mm.

Discussion

The results of our study indicate that contrast-enhanced MR angiography at 3T performs at least as well as 3D TOF-MRA for detection and evaluation of intracranial aneurysms. The requirement to image the cranial arteries quickly on first pass, before major venous enhancement, has previously forced a substantial compromise in spatial resolution relative to TOF-MRA.

Parallel imaging[7-9] offers the ability to greatly increase the speed, coverage, and spatial resolution of first-pass contrast-enhanced MRA. The increased scanning efficiency can be used flexibly to increase spatial and temporal resolution and to increase coverage. However, the SNR penalty associated with parallel acquisition is ultimately limiting as acceleration factors increase, mainly on the basis of the degree of *k*-space undersampling and the coil-array geometry.[7] The higher baseline SNR at 3T can be used to offset the SNR penalty and to support highly accelerated parallel acquisition in the evaluation of cerebrovascular disease.[10,11]

The combination of 3T and highly accelerated parallel acquisition (GRAPPA ×4) enabled us to achieve a high spatial resolution ($0.7 \times 0.6 \times 0.8$ mm^3) over the entire carotid and vertebrobasilar circulation during a short acquisition time. The intracranial aneurysms in our study population were identified and characterized with diagnostic performance equal or superior (in one third of patients) to TOF-MRA. However, our study population was relatively small, and the results must, therefore, be regarded as preliminary. Larger studies will be necessary before our interim conclusions can be generalized.

In conclusion, TOF and contrast-enhanced MRA perform comparably at 3T for evaluation of intracranial aneurysms. The more aggressive parallel acquisition can be used to improve the spatial resolution and coverage of contrast-enhanced MRA, generating submillimeter voxels (0.33 mm^3) in a 20-second acquisition, without the sensitivity to saturation or flow effects characteristic of TOF techniques.

References

1. Stock KW, Radue EW, Jacob AL, et al. **Intracranial arteries: prospective blinded comparative study of MR angiography and DSA in 50 patients.** *Radiology* 1995;195:451–56
2. White PM, Wardlaw JM, Easton V. **Can noninvasive imaging accurately depict intracranial aneurysms? A systematic review.** *Radiology* 2000;217:361–70
3. Isoda H, Takehara Y, Isogai S, et al. **MRA of intracranial aneurysm models: a comparison of contrast-enhanced three-dimensional MRA with time-of-flight MRA.** *J Comput Assist Tomogr* 2000;24:308–15
4. Lin W, Tkach JA, Haacke EM, et al. **Intracranial MR angiography: application of magnetization transfer contrast and fat saturation to short gradient-echo, velocity-compensated sequences.** *Radiology* 1993;186:753–61
5. Metens T, Rio F, Baleriaux D, et al. **Intracranial aneurysms: detection with gadolinium-enhanced dynamic three-dimensional MR angiography—initial results.** *Radiology* 2000;216:39–46
6. Suzuki IM, Matsui, Ueda F, et al. **Contrast-enhanced MR angiography (enhanced 3-D fast gradient echo) for diagnosis of cerebral aneurysms.** *Neuroradiology* 2002;44:17–20
7. Pruessmann KP, Weiger M, Scheidegger MB, et al. **SENSE: sensitivity encoding for fast MRI.** *Magn Reson Med* 1999;42:952–62
8. Sodickson DK, Manning WJ. **Simultaneous acquisition of spatial harmonics (SMASH): fast imaging with radiofrequency coil arrays.** *Magn Reson Med* 1997;38:591–603
9. Griswold MA, Jakob PM, Heidemann RM, et al. **Generalized autocalibrating partially parallel acquisitions (GRAPPA).** *Magn Reson Med* 2002;47:1202–10
10. Nael K, Michaely HJ, Villablanca P, et al. **Time-resolved contrast-enhanced magnetic resonance angiography of the head and neck at 3.0 Tesla: initial results.** *Invest Radiol* 2006;41:116–24
11. Nael K, Ruehm SG, Michaely HJ, et al. **High spatial-resolution CE-MRA of the carotid circulation with parallel imaging: comparison of image quality between 2 different acceleration factors at 3.0 Tesla.** *Invest Radiol* 2006;41:391–99